









RESEARCH ARTICLE | OCTOBER 04 2023

Ion detector of time-of-flight mass spectrometer with registration of leading and trailing edges

V. V. Filatov ; S. V. Filatov ; A. R. Pikhtev ; H. Zhu ; I. V. Sulimenkov ; Z. Huang; V. S. Brusov ; V. I. Kozlovskiy  



Rev. Sci. Instrum. 94, 103303 (2023)


<https://doi.org/10.1063/5.0160716>




View
Online




Export
Citation



Lock-in Amplifier



Boxcar Averager



Zurich
Instruments

Find out more

Boost Your Optics and
Photonics Measurements

Ion detector of time-of-flight mass spectrometer with registration of leading and trailing edges

Cite as: Rev. Sci. Instrum. 94, 103303 (2023); doi: 10.1063/5.0160716

Submitted: 5 June 2023 • Accepted: 14 September 2023 •

Published Online: 4 October 2023



V. V. Filatov,¹ , S. V. Filatov,^{1,2} , A. R. Pikhteleev,¹ , H. Zhu,³ , I. V. Sulimenkov,¹ , Z. Huang,⁴ , V. S. Brusov,¹ , and V. I. Kozlovskiy^{1,a)}

AFFILIATIONS

¹ Chernogolovka Branch of the N.N. Semenov Federal Research Center for Chemical Physics, Russian Academy of Sciences, Prospect Ac. Semenov 1/10, Chernogolovka, Moscow Region 142432, Russia

² Osipyan Institute of Solid State Physics Russian Academy of Sciences, Chernogolovka, 2 Academician Osipyan Str., Moscow Region 142432, Russia

³ Kunshan Hexin Mass Spectrometry Technology Co., Ltd., Kunshan 215311, China

⁴ Institute of Mass Spectrometry and Atmospheric Environment, Jinan University, Guangzhou 510632, China

^{a)} Author to whom correspondence should be addressed: vikozlovskiy@gmail.com

ABSTRACT

The accuracy of the ion flight time measurement in the time-of-flight mass spectrometer is critical to achieving high resolution. The pulse amplitude variation of the detector pulses leads to the registration time spread at a given pulse detection threshold. This time spread can be eliminated by determining the position of the pulse apex. To determine the position of the pulse apex, the output of the ion detector is fed simultaneously to the two channels of the time-to-digital converter. In this case, the first channel is set to register the leading edge, and the second channel is set to register the trailing edge of the pulse. Using a simple processing of the received data, the position of the pulse tip is determined. Thus, the dependence of the temporal position of the peak on the pulse amplitude is largely eliminated. Examples are given, and the efficiency of using this algorithm to increase the resolution of time-of-flight mass spectral peak registration is demonstrated.

Published under an exclusive license by AIP Publishing. <https://doi.org/10.1063/5.0160716>

INTRODUCTION

The resolving power (resolution) is one of the most important characteristics of mass spectrometers. For a time-of-flight mass spectrometer, where the starting energy of ions is given by the potential difference in which they are accelerated, the relative resolution $T/\Delta T$ (temporal) or $M/\Delta M$ (mass) is usually used. Here ΔT and ΔM are the peak widths at half-height in the mass spectrum for the time and mass scales, respectively, and T and M are the recorded ion flight time and mass. The ion flight time in a time-of-flight mass spectrometer is proportional to the square root of the mass-to-charge ratio of the ion, so the mass resolution is half the time resolution, $M/\Delta M = T/2\Delta T$.¹ It is clear that to increase the resolution of the mass spectrometer, it is necessary to minimize the value of ΔT or increase T . The width of the peak registered in the mass spectrum (ΔT or ΔM) is the result of several factors that can be conditionally divided into two groups. The first group includes the variation of ion arrival time determined by the characteristics of the mass analyzer and ion beam parameters. The second group includes the time

uncertainty of the detector response to the ion arrival, determined by the parameters of the detector and the registration system. The present paper is devoted to reducing this uncertainty. The influence of detector and registration system parameters on resolution has been discussed in detail elsewhere.^{2–4} The ion detector of time-of-flight mass spectrometers based on microchannel plates (MCP) has its origins in atomic physics and accelerator engineering,^{5,6} and is also widely used in space research.⁷ Typically, such a detector consists of one, two, or three MCPs in a chevron configuration^{8–11} The output signal of the detector is a short (0.3–2.0 ns) pulse with an amplitude ranging from units to several tens of millivolts. Registration of pulses from the detector output can be performed either by an analog-to-digital converter (ADC) or a time-to-digital converter (TDC).^{12–14}

The use of ADC allows for obtaining a larger dynamic range, which is very much in demand in time-of-flight devices with laser ion sources, electron impact sources, and plasma ion sources.¹⁴ However, the application of ADCs is usually associated with the processing of large datasets. For example, with a detector output pulse

width of 1 ns, a sampling rate of about 5 Gsamples/s is desirable. With an 8-bit ADC, the data stream would be 5 Gbytes/s. To handle such a data stream, it is common to use Field-Programmable Gate Array (FPGA) pre-processing. With relatively simple processing (adding many individual spectra into one), the resolution will be limited by the detector output pulse width. More detailed processing to obtain higher resolution (not limited by the detector output pulse width) may involve identifying peaks and determining their center points for each spectrum.^{15,16} Such processing requires significant FPGA programming efforts or an essential acceleration of the data transfer from the ADC to the computer, in order to perform the processing using personal computer resources.

TDC, in comparison with ADC, has a smaller dynamic range, but allows for acquiring the arrival time of pulses from the detector with higher accuracy. TDC has traditionally been used in particle accelerators and atomic physics experiments where the number of events is small. The accuracy and time resolution of TDCs have always been higher than those of fast ADCs. For example, in the late 1980s, TDC devices with time resolution in fractions of a nanosecond were available, while fast ADCs had a sampling rate of ~ 100 – 500 Msamples/s. The dynamic range with TDC can be increased to some extent by using a detector design with multiple anodes.^{17,18} In the TDC used in our work, the time step of the measured pulse arrival time is 12.8 ps. The output data stream from TDC compared to ADC is 4–5 orders of magnitude smaller, which allows data to be input into a computer in real time, without the use of intermediate accumulation and processing by FPGA means. Real-time registration is important for monitoring fast processes.¹⁹

When using the TDC as a pulse detector, two problems hinder the achievement of high resolution. Both problems are caused by the fact that the pulses from the MCP detector usually vary significantly in amplitude. Many efforts in the development of microchannel plate detector designs are aimed at making the pulse amplitude distribution narrower, or at least different from the exponential distribution with a maximum near the zero pulse amplitude.^{8,10,11}

The first problem is related to the fact that the pulse edges have a finite width. Thus, at a fixed threshold of TDC triggering, the dispersion of pulse amplitudes turns into the dispersion of their registration time. This leads to a deterioration of the mass spectrometer resolution. The second problem is related to the performance of the TDC used. The TDCs we used (E & G Ortec and Cronologic), although having a small time step (100 and 12.8 ps), nevertheless have a noticeable dependence of the response time on the pulse amplitude in case where the ratio of the registration threshold to the pulse amplitude remains the same. For them, it was experimentally found that at small pulse amplitudes, there are shifts in actuation time reaching 400 ps. The resulting variation of the TDC response time will occur even at very steep pulse edges. This variation in the TDC response time also leads to resolution degradation.

These problems can be solved by hardware design improvements. The TDC response time dispersion arising due to the fact that the pulse edges have a finite width can be reduced by decreasing the pulse width from the detector.^{18,20,21} In addition, the effect of the pulse width from the detector can be reduced by increasing the ion transit time in the mass spectrometer. This idea is used in multi-turn time-of-flight mass spectrometers,^{22–24} where the high resolution achieved, again, may be limited by the finite pulse width of the detector.

To avoid time spread when registering the pulse by a constant threshold, the detector output pulse can be made bipolar, and the threshold can be set close to zero. The position of the zero line crossing point does not depend on the pulse amplitude. In this way, it is possible to reduce the variation in registration time due to differences in pulse amplitudes. This method is used in a device called the Constant Fraction Discriminator (CFD). There are many implementations of the CFD.^{25–34} This device is traditionally used in experimental particle physics, as well as in mass spectrometric techniques for space research, when ion flight times are small and high accuracy of pulse registration of different amplitudes is required. Note, however, that this method works well for pulses of similar and known shapes.

The negative effect of both factors can be minimized by producing a discriminator that would isolate pulses in the desired amplitude range. Such a discriminator will lead to a decrease in the dispersion of the registration time in any case, but at the same time, it will reduce the number of registered ions, reducing the sensitivity and dynamic range of the mass spectrometer. The disadvantage of hardware methods can be considered to be their dependence on the parameters of the detector output pulse, such as its width, shape, and polarity.

In this paper, we describe a pulse registration method based on the determination of two parameters for each pulse—the TDC response times for the leading and trailing edges of the pulse, with subsequent processing of the acquired data by software. The described method allowed us to significantly reduce the error of the detector pulse registration time associated with the pulse amplitude spread.

METHODS

In the present work, we used a time-of-flight mass spectrometer described in Ref. 35. The effective ion flight path was 3.4 m. The accelerating voltage was equal to -8 kV. A homemade detector consisting of two MCPO B25-10u (BASPIK Company) in a chevron configuration with a channel diameter of $10\text{ }\mu\text{m}$ and an angle of inclination of the channels to the normal of 12° was used as a detector. The diameter of the anode was 9 mm. The block diagram of the detector is shown in Fig. 1.

The input MCP was under the potential of the ion drift region. The signal from the detector anode was fed to the amplifier input through a high-voltage decoupling and amplified by a homemade amplifier with a bandwidth of 1.2 GHz. A typical oscillogram (oscilloscope LeCroy LC334A) of the pulse from the detector output is

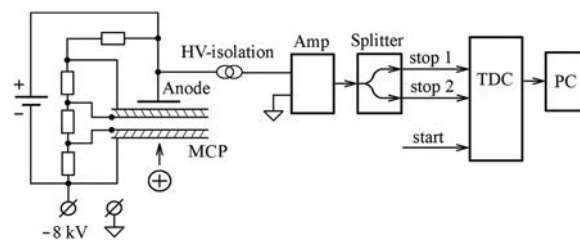


FIG. 1. Block diagram of the mass spectrometer's detector.

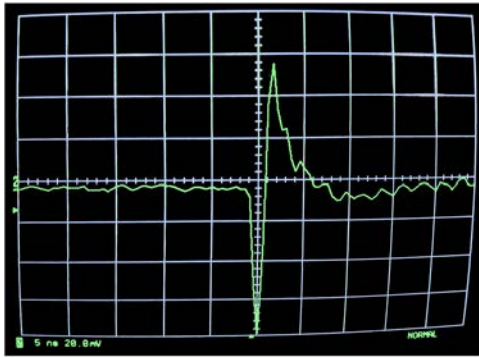


FIG. 2. The mass spectrometer detector output pulse.

shown in Fig. 2. It can be seen that this pulse is bipolar, but only its negative half-wave was the working part of the pulse.

The recording device was a four-channel TDC (xTDC4-PCIe), manufactured by Cronologic. The detector output signal after amplification was divided into two identical channels and fed to two TDC inputs. The triggering of the first TDC channel was set to the leading edge of the signal, and the triggering of the second channel was set to the trailing edge. The registration thresholds were set equal. All events registered by the TDC were recorded in the computer memory and were used to construct mass spectra (histograms) in the process of registration.

When constructing the mass spectrum, the time t , which corresponds to the apex of the detector output pulse, was calculated. Since the working part of this pulse (Fig. 2) was its negative half-wave, the apex of the pulse in this case meant the point of its minimum. The position of the pulse apex does not depend on its amplitude, so the spectrum constructed in this way will not contain the error associated with the transformation of the pulse amplitude spread into its registration time spread. Let us denote the registration time of the pulse leading edge as t_1 and the registration time of the trailing edge as t_2 . If the signal form is symmetrical, the time t calculated by the formula $t = (t_1 + t_2)/2$ will correspond to the apex of the pulse. A real pulse can have different rise and fall times, so the apex of the pulse will not be in the middle, but will be shifted to a steeper edge of the pulse. To account for this, use the expression

$$t = (t_1 + t_2)/2 + \alpha(t_2 - t_1)/2, \quad (1)$$

where α is an experimentally chosen parameter. When $\alpha = -1$, this expression equals t_1 , when $\alpha = 1$, it equals t_2 , and when $\alpha = 0$, it equals $(t_1 + t_2)/2$. Thus, by changing the parameter α , we can register the apex of the pulse also in the case when it is shifted to any side due to the asymmetry of the pulse.

In addition, at the construction of the spectrum (histogram) we chose only those values of t_2 and t_1 , for which the condition was fulfilled

$$T_{\min} < t_2 - t_1 < T_{\max} \quad (2)$$

where T_{\min} and T_{\max} are preset values—the minimum and maximum allowed values of $t_2 - t_1$ difference. For a fixed threshold, the larger $t_2 - t_1$ value will be for pulses of larger amplitude. Therefore,

by limiting the possible range of $t_2 - t_1$, we get a program discriminator of pulse amplitude. By limiting the range of pulse amplitudes in this way, we automatically reduce the scatter of pulse registration times, which contributes to increasing the resolution of the device.

In addition, knowing the value of $t_2 - t_1$, we can distinguish (and take it into account when constructing the spectrum) the arrival of several ions simultaneously on the MCP, because at the same threshold of registration pulses from the arrival of several ions will have a larger value of $t_2 - t_1$. For this purpose, the correspondence between the value of $t_2 - t_1$ and the pulse amplitude should be established beforehand.

Note that both determining the apex of the pulse by correctly setting the parameter α , and discriminating the pulse amplitude by limiting the range of the $t_2 - t_1$ value, should independently lead to improved resolution, and taking into account the value of $t_2 - t_1$ can be used to increase the dynamic range.

Testing of the algorithm

To test the operation of the described algorithm, we made a generator of short pulses, operating at a frequency of 45 kHz. The generator had two outputs—one for start pulses (to synchronize TDC) and the other for stop pulses. The amplitude and width of the stop pulses from the generator corresponded approximately to the pulses from the output of the mass spectrometer detector. The oscillogram of the generator output pulse (Tektronix MSO 4104 oscilloscope) is shown in Fig. 3.

The stop pulses of the generator were fed simultaneously to two TDC channels. One of the channels recorded the leading edge of the pulse, the other—the trailing edge. Figure 4 shows the constructed test spectrum at three values of the parameter α . The leftmost and rightmost curves are the spectra of the signal registered, respectively, by the leading ($\alpha = -1$) and trailing ($\alpha = 1$) edges of the signal. The central curve is the constructed spectrum at $\alpha = 0$.

To illustrate the work of the algorithm as a discriminator of pulse amplitudes (widths), a spectrum was taken in conditions where the output of the generator was connected to the input of TDC through different attenuators. Thus, a spectrum was obtained in which pulses of four different amplitudes were present in equal amounts—0.45, 0.29, 0.23, and 0.16 V. The registration threshold was equal to 0.05 V. Using the time window $T_{\max} - T_{\min} = 13$ ps, the dependence of the number of recorded pulses on the position of

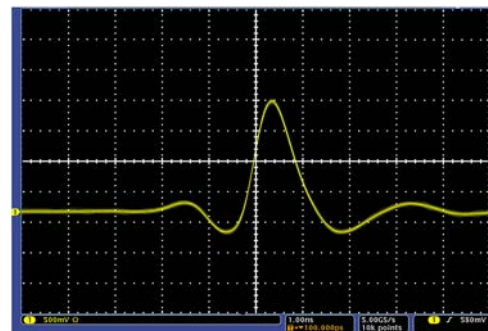


FIG. 3. Output stop pulse of the generator.

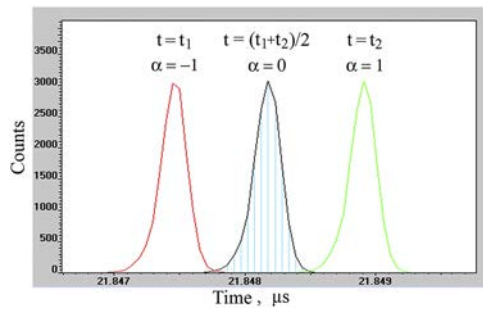


FIG. 4. Test spectra of the generator pulse at different values of the parameter α . The leftmost curve corresponds to the value $\alpha = -1$, the center curve corresponds to the value $\alpha = 0$, and the rightmost curve corresponds to the value $\alpha = 1$.

the middle of this time window $(T_{\min} + T_{\max})/2$ was plotted. This dependence is shown in Fig. 5.

It can be seen that pulses of different amplitude and, therefore, having different values of $t_2 - t_1$ are completely separated. In the case of real spectrum registration, using a fixed threshold, the pulses with different $t_2 - t_1$ values will correspond to pulses with different amplitudes. Thus, this algorithm will work as a program amplitude discriminator.

The TDC response time may depend on the pulse amplitude and the detection threshold, as well as on their ratio. It may be different when registering the leading and trailing edges of the pulse, as well as at different polarities of the pulse. To find out the role that such a delay in the registration time can play, the following experiment was conducted. The pulse spectrum of the test oscillator was filmed at different pulse amplitudes. The pulse was attenuated by attenuators 0, 3, 6, 10, and 12 dB. The pulse amplitudes were 0.9, 0.637, 0.451, 0.285, and 0.226 V, respectively. The registration

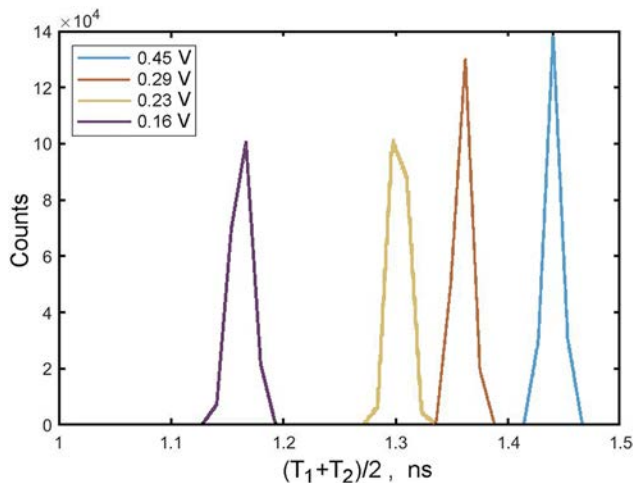


FIG. 5. Test spectrum illustrating the operation of the algorithm as an amplitude discriminator. The spectrum represents the dependence of the number of registered pulses on the position in the middle of the time window $(T_{\min} + T_{\max})/2$. The width of the time window $T_{\max} - T_{\min}$ was equal to 13 ps. The spectrum sections corresponding to different amplitudes of the input signal are marked in color.

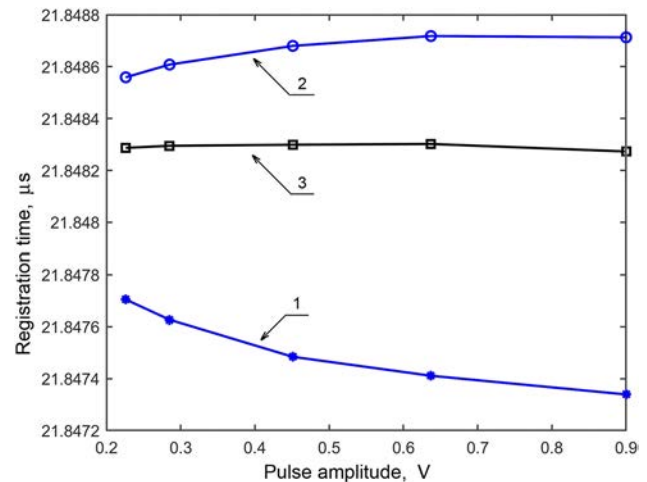


FIG. 6. Dependences of the registration time of the leading (1) and trailing (2) edges of the pulse, as well as the time calculated at $\alpha = 0.35$ (3), on the pulse amplitude. The registration threshold is 0.1 V.

threshold was equal to 0.1 V. The dependences of the registration time of the leading and trailing edges of the pulse on the pulse amplitude were plotted. At the same time, a correction was made for the time of signal propagation in the attenuators. This time was measured separately with an ADVANTEST R3762A vector circuit analyzer. The error of the propagation time measurement did not exceed 5 ps. The results are shown in Fig. 6.

From Fig. 6 shows that the change in registration time at different pulse amplitudes for the leading edge (1) is greater than for the trailing edge (2). However, since our stop pulse has a steeper leading edge than the trailing edge (Fig. 3), we should have expected the opposite. This seems to be explained by the fact that, for the leading edge, the dependence of the time of its registration on the amplitude, which is due to the imperfection of the TDC, is larger than for the trailing edge. The curves 1 and 2, shown in Fig. 6, are a consequence of two different factors: the finite rise/fall times of the pulse fronts and the different delay times for their registration. The influence of these two factors does not allow us to choose the parameter α based only on the shape of the observed pulse. The parameter α has to be determined empirically. Figure 6 also shows a graph of the dependence of the calculated registration time on the pulse amplitude at the best value of the parameter α (curve 3). The maximum variation of the registration time of curve 3 (29 ps) is 5.5 times smaller than that of curve 2 (159 ps) and 11.5 times smaller than that of curve 1 (366 ps). Thus, we can conclude that the use of this algorithm allows us to significantly (five times) reduce the registration time spread. Moreover, this algorithm is also effective in the case when we are dealing with the mixed effect of two different factors at this time: the finite rise/fall times of the pulse fronts and different delay times during their registration.

Experimental results

To verify the operation of the described algorithm on a real spectrum, we recorded the mass spectrum of Gramicidin S using an

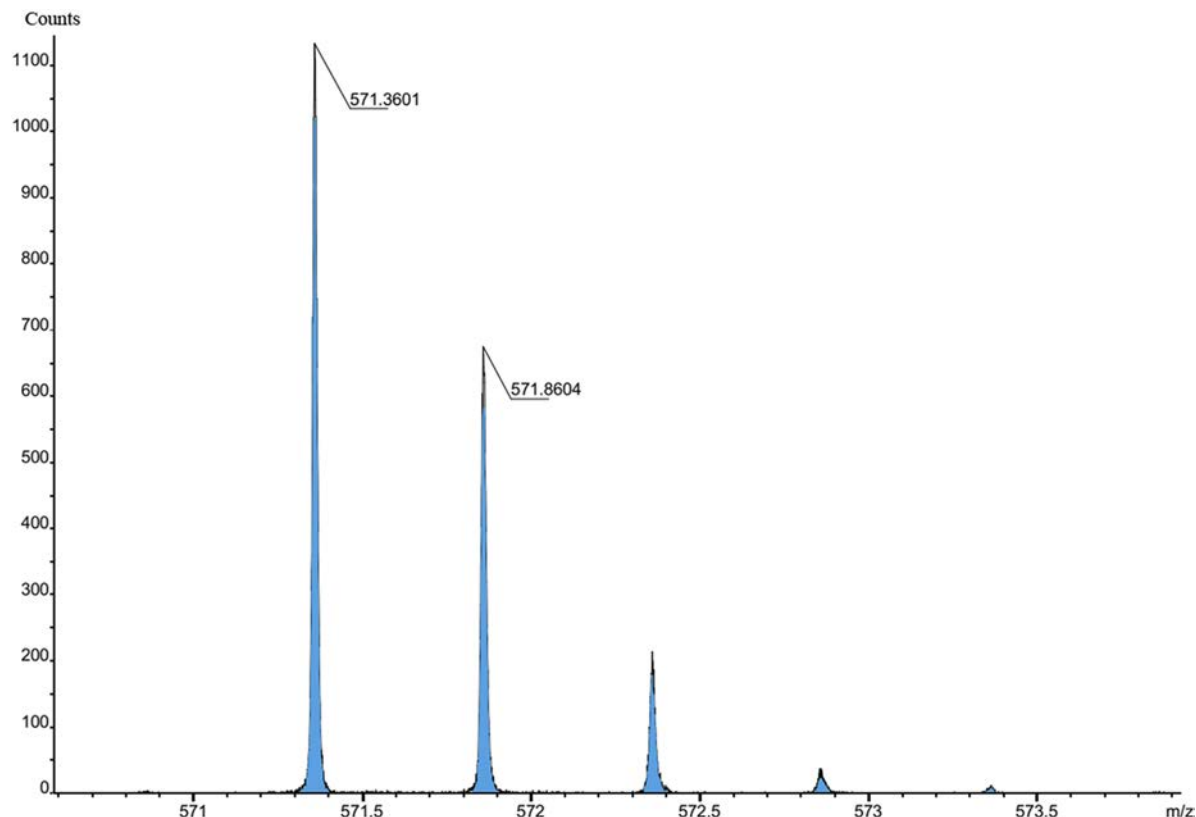


FIG. 7. The region of the mass spectrum containing the double protonated Gramicidin S ions $[M + 2H]^{2+}$.

electrospray ion source. Figure 7 shows the isotopic pattern of the double protonated Gramicidin S ion $[M + 2H]^{2+}$.

The following Figs. 8–10 are plotted using the same ion arrival times (leading and trailing edges) for 90 ss of Gramicidin S electrospray registration. Using these data, one can then construct mass spectra (histograms) for any selected values of T_{\min} , T_{\max} , and α .

Figure 8 shows the dependences of mass resolution (1 and 2) and ion current (3) on the $T_{\max} - T_{\min}$ time window width for the main isotopic peak of Gramicidin S ($m/z = 571.36$).

The position of the middle of the time window $(T_{\max} + T_{\min})/2$ was chosen to be 1.25 ns. Zero on the time axis corresponds to the values $T_{\max} = T_{\min} = 1.25$ ns. Other values on the time axis are $T_{\max} - T_{\min}$ values obtained by simultaneously increasing the value of T_{\max} and the same decrease in T_{\min} . It can be seen that the ion current (curve 3) saturates when $T_{\max} - T_{\min}$ increases to 2.5 ns, i.e., the widths of almost all pulses are in a range of 0–2.5 ns.

Curve 1 is the dependence of the resolution on the value of $T_{\max} - T_{\min}$ at $\alpha = -1$. At this value of the parameter α , the detector pulses are registered exclusively by their leading edge. It can be seen that when the time window is narrowed, the mass resolution increases from 39 000 to 56 000. This is explained by the fact that at small values of $T_{\max} - T_{\min}$, the pulses of close amplitudes are selected for spectrum construction; hence, the corresponding

registration time scatter is also small, which leads to an increase in resolution.

Curve 2 is the dependence of the resolution on the time window value at $\alpha = -0.2$. Narrowing the time window in this case leads to an increase in resolution from 47 000 to 58 000. Curve 2 is located above curve 1, i.e., the resolution at $\alpha = -0.2$ is greater than the resolution at $\alpha = -1$ for all values of the time window.

Figure 9 shows, for the same experimental data, the dependences of resolution on the parameter α for three values of the time window $T_{\max} - T_{\min}$: 3.5, 1.1, and 0.5 ns.

It can be seen that with the time window $T_{\max} - T_{\min} = 3.5$ ns, the resolution depends quite strongly on the parameter α . The resolution reaches a maximum of 47 000 at $\alpha = -0.2$, equals 39 000 at $\alpha = -1$, and is only 35 000 at $\alpha = 1$. With a time window of $T_{\max} - T_{\min} = 1.1$ ns, the resolution is higher, and it is less dependent on the parameter α . When $T_{\max} - T_{\min} = 0.5$ ns, the resolution is even higher and almost independent of the parameter α .

Note that Figs. 8 and 9 show the effect of decreasing resolution when the time window width increases at the optimal value of the parameter α ($\alpha = -0.2$), although it would seem that resolution should remain maximal and not depend on the time window width.

This effect could be explained by the fact that, with a wide time window, we are dealing with a large scatter of pulse amplitudes. Under these conditions, the quality of our algorithm could have

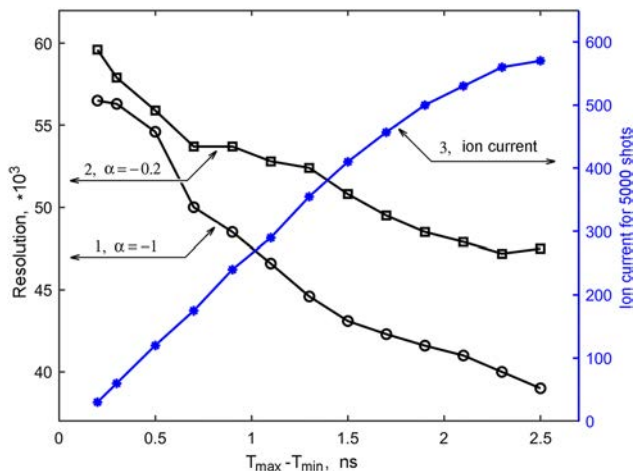


FIG. 8. Dependences of the mass resolution (1 and 2) and ion current (3) on the $T_{\max} - T_{\min}$ time window for the main Gramicidin S isotopic peak ($m/z = 571.36$). The mass resolution is presented at two values of the parameter α : $\alpha = -1$ (1) and $\alpha = -0.2$ (2). The position of the middle of the time window $(T_{\max} + T_{\min})/2$ is 1.25 ns. The registration threshold is 0.7 V.

deteriorated. To test this version, a term quadratic to $(t_2 - t_1)$ was included in the formula for calculating the time t , which corresponds to the pulse apex,

$$t = (t_1 + t_2)/2 + \alpha \cdot (t_2 - t_1)/2 + \beta \cdot (t_2 - t_1)^2, \quad (3)$$

where β is the second parameter to be selected. However, by selecting the parameter β , it was not possible to increase the resolution and explain the observed effect in this way. Although in other parts of the spectrum (at smaller values of the registration threshold), the selection of the parameters α and β succeeded in obtaining greater resolution than when only one parameter α was selected.

To elucidate the cause of the above effect, we plotted the dependences of ion current and resolution on the position of the middle of

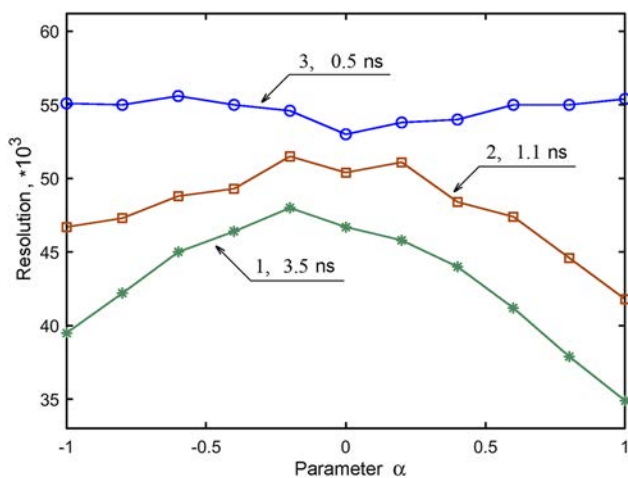


FIG. 9. Dependences of resolution on the parameter α for three values of $T_{\max} - T_{\min}$: 3.5 ns (1), 1.1 ns (2) and 0.5 ns (3).

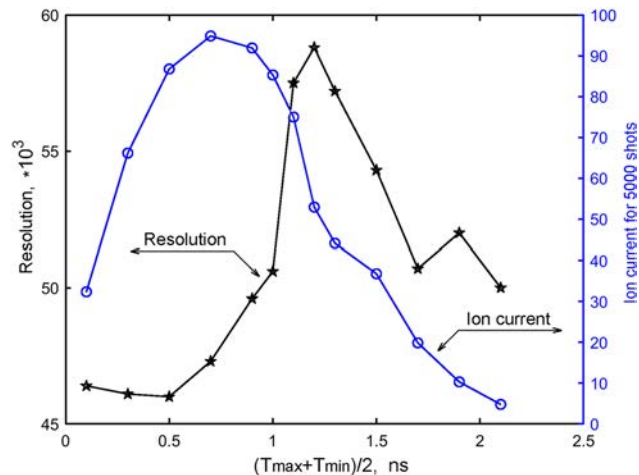


FIG. 10. Dependences of ion current and resolution on the position of the middle of the time window $(T_{\max} + T_{\min})/2$ with its fixed width $T_{\max} - T_{\min} = 0.2$ ns.

the $(T_{\max} + T_{\min})/2$ time window, the width of which was taken to be $T_{\max} - T_{\min} = 0.2$ ns. These dependences are shown in Fig. 10.

It can be seen that the ion current reaches its maximum at a detector pulse width of 0.7 ns, while the resolution has a maximum (58 000) at a detector pulse width of 1.2 ns, when the ion current has already decreased by a factor of 1.7. This can be explained by assuming, that in our case, two or more ions arrive at the MCP simultaneously. In this case, there is an increase in the amplitude (and, accordingly, the width of the detector pulses), as well as averaging of the arrival times of ions. The averaging of the ion arrival times leads to an increase in the resolution. This is consistent with the fact that when using an MCP with a channel diameter of 10 μm and an angle of 12° , the limiting resolution due to these MCP parameters for our mass spectrometer, which has an effective ion flight length of 3.4 m, will be about a value of 50 000. I.e., an increase in resolution greater than 50 000 under our conditions can be obtained only by averaging the time of registration during the simultaneous arrival of two or more ions. Increasing the width of the time window (Fig. 8) at its central value of 1.25 ns mainly includes single arrivals (Fig. 10), for which the resolution is smaller, so the resolution decreases when the time window is increased. The decrease in resolution at time window positions greater than 1.3 ns (Fig. 10) is apparently due to the fact that at larger pulse widths, the value of the parameter α ceases to be optimal. The low signal-to-noise ratio in this region does not allow us to draw an unambiguous conclusion.

In the present work, the considered algorithm was analyzed on the example of the most intense peak in the mass spectrum—the main isotopic peak of the double charged Gramicidin S ions ($[M + 2H]^{2+}$, $m/z = 571.36$). In order to understand whether this algorithm would be applicable over a wide range of m/z , the resolution dependences on the parameter α for both the double- and single-charged Gramicidin S ions were plotted in Fig. 11.

In order not to limit the ion current and to take into consideration, as far as possible, all the pulses registered by TDC, the values of $T_{\max} - T_{\min}$ in this case were taken in a wide range (from 0.1 to 3.5 ns), and the registration threshold was taken as minimal (0.1 V).

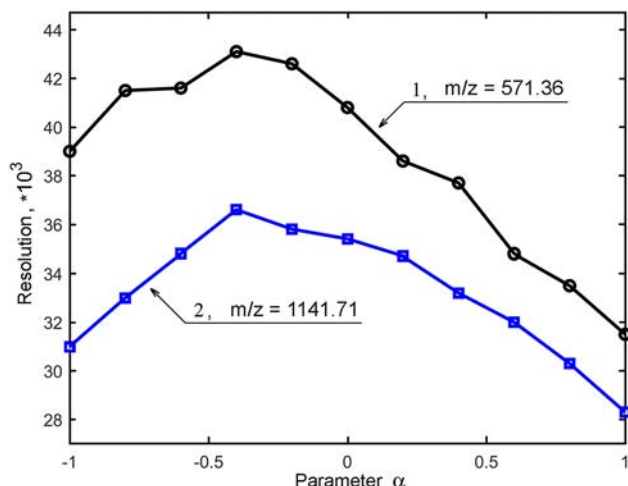


FIG. 11. Resolution dependences on the parameter α for the main isotopic peaks of the double-charged (1, $m/z = 571.36$) and single-charged (2, $m/z = 1141.71$) Gramicidin S ions. The range of values of the time window $T_{\max} - T_{\min}$ was chosen from 0.1 to 3.5 ns, and the threshold of registration was 0.1 V.

Figure 11 shows that in both cases, the resolution increases when the parameter α value is in the range $(-0.5, -0.2)$ compared to the resolution at $\alpha = -1$ and $\alpha = +1$. Thus, the considered algorithm is applicable both for double-charged and single-charged ions of Gramicidin S, i.e., for m/z values differing by a factor of two. Moreover, the optimal value of α is approximately the same for these two m/z values. The absence of an explicit dependence of the optimal value of α on the m/z value allows us to choose the parameter α using the intense peaks of the spectrum and use this choice for the whole mass spectrum.

The optimal value of the parameter α should be sensitive to the shape of the signal. We believe that, in our case, the shape of the signal depends more on the circuitry of the detector and amplifier and it is not directly related to the m/z value.

CONCLUSION

In this paper, an original ion detector configuration is proposed and realized, and its capabilities are demonstrated using an orthogonal time-of-flight mass spectrometer. Let us note the main points that characterize the advantages of the proposed method of ion arrival time registration: the correct choice of the parameter α and the use of a program discriminator of detector pulse widths (amplitudes) independently lead to an increase in the resolution of the mass spectrometer; the choice of the parameter α allows us to improve the resolution of the mass spectrometer without reducing its sensitivity, and in a wide enough range of m/z values; the use of the program discriminator algorithm allows us to output the already acquired spectrum either with maximum sensitivity or with maximum resolution.

We suppose that pulse width information can be used to increase the dynamic range.

In addition, pulse width (amplitude) discrimination allows us to examine the acquired spectrum for the presence of pulses in a

given range of widths (amplitudes), which is useful, in particular, when analyzing the quality of the MCP.

The proposed algorithm of data processing allowed for an increase in the mass resolution of this mass spectrometer from 39 000 to 58 000. The analysis of experimental data using this algorithm allowed us to establish that the main parameter limiting the resolution in our case is the diameter of the MCP channels.

The use of this algorithm reduces the influence on the mass spectrometer resolution of both the finite rise time of the detector output pulse edge and the dependence of the TDC response time on the pulse amplitude, which can essentially simplify the detector design.

AUTHOR DECLARATIONS

Conflict of Interest

The authors have no conflict of interest to disclose.

Author Contributions

V. V. Filatov: Conceptualization (equal); Data curation (equal); Formal analysis (equal); Investigation (equal); Methodology (equal); Validation (equal); Visualization (equal); Writing – original draft (equal); Writing – review & editing (equal). **S. V. Filatov:** Data curation (equal); Formal analysis (equal); Investigation (equal); Methodology (equal); Software (equal). **A. R. Pikhteleev:** Data curation (equal); Investigation (equal); Software (equal). **H. Zhu:** Funding acquisition (equal); Resources (equal); Validation (equal). **I. V. Sulimenkov:** Formal analysis (equal); Resources (equal); Validation (equal); Writing – review & editing (equal). **Z. Huang:** Formal analysis (equal); Funding acquisition (equal); Resources (equal); Validation (equal); Writing – review & editing (equal). **V. S. Brusov:** Formal analysis (equal); Investigation (equal); Resources (equal). **V. I. Kozlovskiy:** Investigation (equal); Methodology (equal); Supervision (equal); Validation (equal); Writing – review & editing (equal).

DATA AVAILABILITY

The data that support the findings of this study are available from the corresponding author upon reasonable request.

REFERENCES

- ¹A. Radionova, I. Filippov, and P. J. Derrick, "In pursuit of resolution in time-of-flight mass spectrometry: A historical perspective," *Mass Spectrom. Rev.* **35**, 738–757 (2016).
- ²R. J. Cotter, "Time-of-flight mass spectrometry: Basic principles and current state," *ACS Symp. Ser.* **549**, 16–48 (1993).
- ³A. F. Dodonov, I. V. Chernushevich, and V. V. Laiko, *ACS Symp. Ser.* **549**, 108 (1994).
- ⁴J. N. Coles and M. Guilhaus, "Resolution limitations from detector pulse width and jitter in a linear orthogonal-acceleration time-of-flight mass spectrometer," *J. Am. Soc. Mass Spectrom.* **5**(8), 772–778 (1994).
- ⁵H. Wollnik, "Energy-isochronous time-of-flight mass analyzers," *Int. J. Mass Spectrom. Ion Processes* **131**, 387–407 (1994).
- ⁶O. H. W. Siegmund, "High-performance microchannel plate detectors for UV/visible astronomy," *Nucl. Instrum. Methods Phys. Res., Sect. A* **525**(1–2), 12–16 (2004).

- ⁷O. Jagutzki, V. Mergel, K. Ullmann-Pfleger, L. Spielberger, U. Spillmann, R. Dörner, and H. Schmidt-Böcking, "A broad-application microchannel-plate detector system for advanced particle or photon detection tasks: Large area imaging, precise multi-hit timing information and high detection rate," *Nucl. Instrum. Methods Phys. Res., Sect. A* **477**(1–3), 244–249 (2002).
- ⁸J. L. Wiza, "Microchannel plate detectors," *Nucl. Instrum. Methods* **162**, 587–601 (1979).
- ⁹H. Kobayashi, T. Hondo, N. Imaoka, M. Suyama, and M. Toyoda, "Development of novel ion detector that combines a microchannel plate with an avalanche diode," *Nucl. Instrum. Methods Phys. Res., Sect. A* **971**, 164110 (2020).
- ¹⁰O. H. W. Siegmund, K. Coburn, and R. F. Malina, "Investigation of large format microchannel plate Z configurations," *IEEE Trans. Nucl. Sci.* **32**(1), 443–447 (1985).
- ¹¹G. W. Fraser, M. T. Pain, J. E. Lees, and J. F. Pearson, "The operation of microchannel plates at high count rates," *Nucl. Instrum. Methods Phys. Res., Sect. A* **306**(1–2), 247–260 (1991).
- ¹²S. D. Negra, Y. Le Beyec, and P. Håkansson, "Spontaneous desorption time-of-flight mass spectrometry (SDMS): Time correlated emission of electrons and negative ions in a constant electric field," *Nucl. Instrum. Methods Phys. Res., Sect. B* **9**(1), 103–106 (1985).
- ¹³R. D. Macfarlane and D. F. Torgerson, "²⁵²Cf-plasma desorption time-of-flight mass spectrometry," *Int. J. Mass Spectrom. Ion Phys.* **21**(1–2), 81–92 (1976).
- ¹⁴F. Hillenkamp, E. Unsöld, R. Kaufmann, and R. Nitsche, "A high-sensitivity laser microprobe mass analyzer," *Appl. Phys.* **8**, 341–348 (1975).
- ¹⁵J. C. Fjeldsted, A. J. Hidalgo, and W. D. Frazer, "Mass spectrometer and method for enhancing resolution of mass spectra," U.S. patent US7908093B2 (15 March 2011).
- ¹⁶R. H. Bateman, J. M. Brown, M. Green, J. L. Wildgoose, A. J. Gilbert, and S. D. Pringle, "Conversion of ion arrival times or ion intensities into multiple intensities or arrival times in a mass spectrometer," U.S. patent US9673031B2 (06 June 2017).
- ¹⁷K. Fuhrer, M. Gonin, T. F. Egan, W. Burton, J. Albert Schultz, V. E. Vaughn, and S. R. Ulrich, "Fast time-of-flight mass spectrometer with improved dynamic range," U.S. patent US7800054B2 (21 September 2010).
- ¹⁸A. Riedo, M. Tulej, U. Rohner, and P. Wurz, "High-speed microstrip multi-anode multichannel plate detector system," *Rev. Sci. Instrum.* **88**, 045114 (2017).
- ¹⁹K. Fuhrer, M. Gonin, K. J. Gilling, T. F. Egan, M. I. McCully, and A. J. Schultz, "Time-of-flight mass spectrometer for monitoring of fast processes," U.S. patent US0784395B2 (18 October 2004).
- ²⁰P. Wurz and L. Gubler, "Fast microchannel plate detector for particles," *Rev. Sci. Instrum.* **67**, 1790 (1996).
- ²¹R. Schletti, P. Wurz, S. Scherer, and O. H. Siegmund, "Fast microchannel plate detector with an impedance matched anode in suspended substrate technology," *Rev. Sci. Instrum.* **72**, 1634 (2001).
- ²²H. Wollnik, A. Casares, D. Radford, and M. Yavor, "Multi-pass time-of-flight mass spectrometers of high resolving power," *Nucl. Instrum. Methods Phys. Res., Sect. A* **519**(1–2), 373–379 (2004).
- ²³A. Verenchikov, S. Kirillov, Y. Khasin, V. Makarov, M. Yavor, and V. Artaev, "Multiplexing in multi-reflectron TOF MS," *J. Appl. Sol. Chem. Model.* **6**(1), 1–22 (2017).
- ²⁴P. Schury, M. Wada, Y. Ito, D. Kaji, F. Arai, M. McCormick, I. Murray, H. Haba, S. Jeong, S. Kimura, H. Koura, H. Miyatake, K. Morimoto, K. Morita, A. Ozawa, M. Rosenbusch, M. Reponen, P.-A. Söderström, A. Takamine, T. Tanaka, and H. Wollnik, "First online multireflection time-of-flight mass measurements of isobar chains produced by fusion-evaporation reactions: Toward identification of superheavy elements via mass spectroscopy," *Phys. Rev. C* **95**, 011305(R) (2017).
- ²⁵D. A. Gedcke and W. J. McDonald, "A constant fraction of pulse height trigger for optimum time resolution," *Nucl. Instrum. Methods* **55**, 377–380 (1967).
- ²⁶G. J. Wozniak, L. W. Richardson, and M. R. Maier, "Time-walk characteristics of an improved constant fraction discriminator," *Nucl. Instrum. Methods* **180**(2–3), 509–510 (1981).
- ²⁷J. Kostamovaara and R. Myllylä, "A time-to-amplitude converter with constant fraction timing discriminators for short time interval measurements," *Nucl. Instrum. Methods Phys. Res., Sect. A* **239**(3), 568–578 (1985).
- ²⁸M. L. Simpson, G. R. Young, R. G. Jackson, and M. Xu, "A monolithic, constant-fraction discriminator using distributed R-C delay line shaping," in *IEEE Nuclear Science Symposium and Medical Imaging Conference Record* (IEEE, San Francisco, CA, 1995), Vol. 1, pp. 292–296.
- ²⁹S. Cova, M. Ghioni, F. Zappa, and A. Lacaita, "Constant-fraction circuits for picosecond photon timing with microchannel plate photomultipliers," *Rev. Sci. Instrum.* **64**(1), 118–124 (1993).
- ³⁰D. Breton, E. Delagnes, J. Maalmi, K. Nishimura, L. L. Ruckman, G. Varner, and J. Va'vra, "High resolution photon timing with MCP-PMTs: A comparison of a commercial constant fraction discriminator (CFD) with the ASIC-based waveform digitizers TARGET and WaveCatcher," *Nucl. Instrum. Methods Phys. Res., Sect. A* **629**(1), 123–132 (2011).
- ³¹A. Harter, M. Weinert, L. Knafla, J.-M. Régis, A. Esmaylzadeh, M. Ley, and J. Jolie, "Investigating timing properties of modern digitizers utilizing interpolating CFD algorithms and the application to digital fast-timing lifetime measurement," *arXiv:2303.07946* (2023).
- ³²M. Ghioni, S. Cova, C. Samori, and F. Zappa, "True constant fraction trigger circuit for picosecond photon-timing with ultrafast microchannel plate photomultipliers," *Rev. Sci. Instrum.* **68**(5), 2228–2237 (1997).
- ³³J.-F. Genat, G. Varner, F. Tang, and H. Frisch, "Signal processing for picosecond resolution timing measurements," *Nucl. Instrum. Methods Phys. Res., Sect. A* **607**(2), 387–393 (2009).
- ³⁴A. Kilpelä, J. Ylitalo, K. Määttä, and J. Kostamovaara, "Timing discriminator for pulsed time-of-flight laser rangefinding measurements," *Rev. Sci. Instrum.* **69**(5), 1978–1984 (1998).
- ³⁵A. F. Dodonov, V. I. Kozlovski, I. V. Soulimenkov, V. V. Raznikov, A. V. Loboda, Z. Zhen, T. Horwath, and H. Wollnik, "High-resolution electrospray ionization orthogonal-injection time-of-flight mass spectrometer," *Eur. J. Mass Spectrom.* **6**(6), 481 (2000).